

INTERACTION OF LASER RADIATION WITH MATTER

PACS numbers: 21.10.–k; 42.65.Re; 52.38.Ph
DOI: 10.1070/QE2011v041n03ABEH014544

Internal electron conversion of the isomeric ^{57}Fe nucleus state with an energy of 14.4 keV excited by the radiation of the plasma of a high-power femtosecond laser pulse

G.V. Golovin, A.B. Savel'ev, D.S. Uryupina, R.V. Volkov

***Abstract*. We recorded the spectrum of delayed secondary electrons ejected from the target, which was coated with a layer of iron enriched with the ^{57}Fe isotope to 98 %, under its irradiation by fluxes of broadband X-ray radiation and fast electrons from the plasma produced by a femtosecond laser pulse at an intensity of 10^{17} W cm^{-2}. Maxima were identified at energies of 5.6, 7.2, and 13.6 keV in the spectrum obtained for a delay of 90 – 120 ns. The two last-listed maxima owe their origin to the internal electron conversion of the isomeric level with an energy of 14.4 keV and a lifetime of 98 ns to the K and L shells of atomic iron, respectively; the first-named level arises from a cascade $K - L_2L_3$ Auger process. Photoexcitaion by the X-ray plasma radiation is shown to be the principal channel of the isomeric level excitation.**

Keywords: *quantum nucleonics, superstrong light fields, plasma of ultrashort laser pulses, nuclear processes.*

1. Introduction

Hot dense laser-produced plasma is a promising tool for nuclear physical investigations [1 – 3]. Even for a 'moderate' intensity of an ultrashort laser pulse (above 10^{16} W cm^{-2}), this plasma is a source of electrons, ions, and photons with energies of tens of keV [4], and for higher intensities of laser radiation the particle energies are as high as 1 – 50 MeV per nucleon [5]. One of the most interesting and promising lines of research in this area may involve the excitation of isomeric nuclear levels possessing a relatively low energy on the nuclear energy scale or the excitation of levels located close to a long-lived isomeric state [6 – 10]. Known to date are only two experimental works that reported the observation of gamma-ray radiation arising from the relaxation of the excited 76.5-eV level of the ^{235}U isotope and the 6.237-keV level of the ^{181}Ta isotope [7, 11]; however, attempts to reproduce these results did not meet with success [12 – 15].

Recording the relaxation of nuclei excited in a plasma encounters serious experimental difficulties. First, the number of nuclei that experience excitation is extremely low (of the order of $10^{-2} - 1$ per one laser pulse in the plasma volume), which is a consequence of the small width of a nuclear transition. In this case, the plasma is an intense source of broadband X-ray radiation, including the radiation with the photon energy of the order of the nuclear transition energy. This radiation saturates detectors and does not allow commencing measurements of gamma decay earlier than 1 μs after the plasma 'ignition'.

Internal conversion decay channel is the principal one for low-lying nuclear levels and is attended with the ejection of an internal conversion electron by the atom rather than a gamma-ray photon (the typical internal conversion coefficient for these levels ranges from 5 – 10 to tens of thousands). That is why an experimental scheme intended to detect precisely the internal conversion electrons (with energy and time resolution) appears to be substantially more efficient; however, in this case, too, the signal arising from single internal conversion electrons is to be extracted from the strong background of intrinsic plasma electrons.

In the present work we realised a new approach to the investigation of relatively short-lived low-lying isomeric nuclear states, which involved the use of a hot dense laser-produced plasma: the isomeric level was excited outside the plasma in an external target containing a relatively small amount of the isotope under investigation, with the subsequent recording of the electron energy spectrum with temporal resolution. The efficiency of the approach was demonstrated by the example of the ^{57}Fe isotope with a nuclear level energy of 14.41 keV and a lifetime of 98 ns [16].

Recording the internal conversion channel of excited nuclear state decay requires information about the possible energy spectrum of the electrons resulting from this process. In the course of internal electron conversion there occurs ionisation of one of atomic electron shells, and therefore the kinetic energy of the electrons being recorded will be equal to the difference of the isomeric nuclear state energy and the electron binding energy for this shell. To calculate the partial coefficients of conversion to different shells and find the energy spectrum of the internal conversion electrons we took advantage of a code package which realises the Dirac – Fock technique for the calculation of the wave functions of electrons residing in the self-consistent atomic field [17].

Figure 1 shows the results of this calculation for the isomeric state of the ^{57}Fe nucleus with an energy of 14.41 keV. As is evident from Fig. 1, the internal conversion proceeds primarily via the K shell. This signifies that the decay of the excited nuclear state in the majority of cases will give rise to an electron with kinetic energy equal to the

G.V. Golovin, A.B. Savel'ev, D.S. Uryupina, R.V. Volkov Department of Physics and International Laser Centre, M.V. Lomonosov Moscow State University, Vorob'evy gory, 119992 Moscow, Russia; e-mail: deep68@yandex.ru, ab_savelev@phys.msu.ru

Received 17 January 2011; revision received 17 February 2011
Kvantovaya Elektronika **41** (3) 222 – 226 (2011)
Translated by E.N. Ragozin

difference between the nucleus excitation energy (14.41 keV) and the electron binding energy in the K shell (7.1 keV), as well as to a vacancy in this shell. The vacancy will be almost instantly occupied (in several femtoseconds [18]) by electrons from the higher lying shells due to Auger transitions, primarily via the $K - L_2L_3$ and $K - L_3L_3$ channels. As a result, the expected set of electrons ejected from a ^{57}Fe atom in the decay of its first excited nuclear state should contain the electrons arising from ionisation of the shell via which the internal electron conversion proceeds as well as the electrons arising from Auger processes in the ionised atom (Fig. 2).

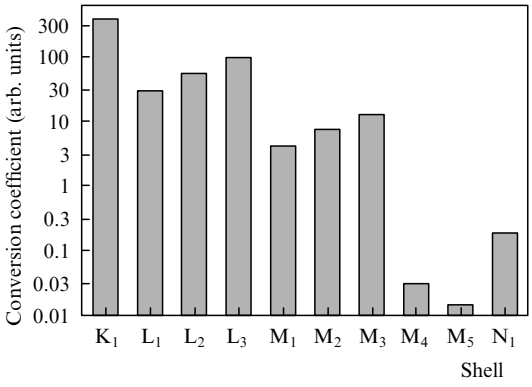

Figure 1. Partial internal conversion probabilities for the isomeric state of the ^{57}Fe isotope with an energy of 14.41 keV.

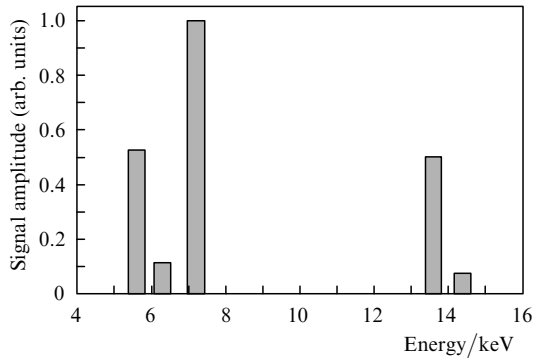

Figure 2. Spectrum of internal conversion and attendant Auger electrons for the ^{57}Fe isotope which arise from the internal electron conversion of the isomeric state with an energy of 14.41 keV.

2. Experiment

The laser-produced plasma in our experiments (Fig. 3) was generated by Ti : sapphire laser radiation (the pulse duration and energy: 50 fs and 1.5 mJ), which was focused at an angle of 45° onto the surface of a thick steel plate with an aberration-free lens ($F/D \approx 6$) to a spot approximately 4 μm in diameter (intensity in the focal spot: $\sim 10^{17}$ W cm^{-2}). The radiation contrast ratio was no worse than 2×10^{-7} on the nanosecond scale and was defined by a short prepulse which leaked from the regenerative amplifier. On the picosecond scale, the contrast ratio was defined by a short prepulse with a relative amplitude of 3×10^{-5} with an advance of 23 ps [19].

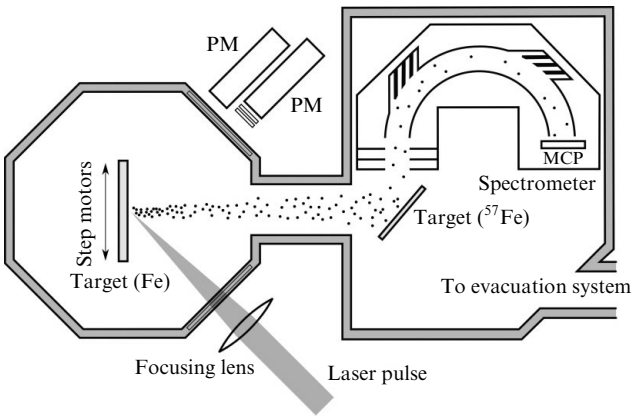

Figure 3. Experimental facility.

The average energy of the X-ray radiation (and, hence, of the hot electrons) of the resultant plasma was measured for every pulse by the filter technique using two PMs with 5-mm-thick Na I scintillators [20] and was equal to 11 ± 2 keV. After every laser pulse the target was shifted, so that the radiation interacted with a plane surface rather than with a crater remaining after the previous shot. The electrons and ions accelerated in the plasma along the normal to the surface of the primary target bombarded the secondary target, which was located at a distance of 27 cm from the primary one. The secondary target was a silicon plate with a surface area of about 1 cm^2 coated with a thin (200 nm) layer of iron enriched with a ^{57}Fe isotope to a density of 98 %. Additional measurements revealed that the average electron energy was equal to 13 ± 1 keV and the ion energy to 26 ± 3 keV per charge [21]. The angle of particle incidence on the secondary target was equal to about 45°. The electrons knocked out of this target passed through the deflecting plates of an electrostatic spectrometer [20], whose entrance window (2 by 0.5 cm) was spaced at 4 cm from the secondary target, and recorded with a VEU-7 chevron-type microchannel plate (MCP). The secondary target and the electron spectrometer were located in a separate vacuum chamber connected vacuum-tightly to the interaction chamber. By varying the voltage across the spectrometer plates, we changed the energy of recorded particles in the range from 4 to 20 keV per unit charge, while the polarity of the voltage applied to the plates defined the sense of the charge of the particles being recorded. The energy resolution of the spectrometer was determined primarily by its geometry and was equal to 10 %. A vacuum of 10^{-5} Torr was maintained in the chambers which accommodated both targets and the spectrometer. The electron current from VEU-7 was recorded with the aid of an ADC PLX9054 PCI PC card (Rudnev-Shilyaev corporation) with a digitisation frequency of 500 MHz and an 8-bit resolution.

Figure 4 shows the typical signal acquired in one laser shot from the VEU-7 detector with the spectrometer recording electrons. This signal was subjected to filtration procedure: a signal averaged over several thousands of the same signals was subtracted from it in order to eliminate the slowly varying contribution arising from the parasitic pick-up signal. In Fig. 4, the 'noise' for delays from 0 to 50 – 90 ns after the instant of plasma production is due to the fact that VEU-7 recorded the flux of 'hot' electrons from the

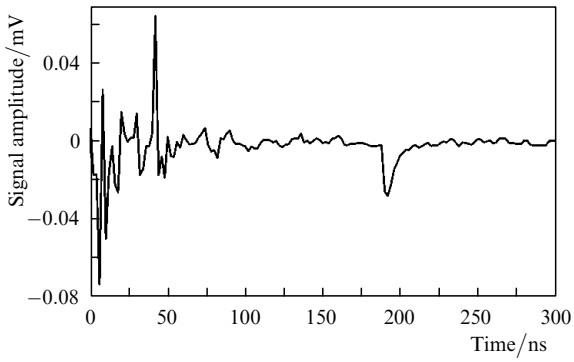

Figure 4. Typical signal recovered from the VEU-7 detector when recording electrons.

plasma, which were scattered by the secondary target in the direction of the entrance spectrometer window. The peak of characteristic shape (a sharp front and a gentle slope) observed at a delay of 190 ns corresponds to the detection of a single electron.

3. Data processing and discussion of results

For each energy of recorded electrons we executed about 10000 measurements and counted all events arising from the detection of single electrons in each of them. Figure 5 shows the typical time dependence of the average electron current. One can clearly see the maxima emerging with delays of 120 – 200, 500 – 600, and 675 – 750 ns relative to the instant of plasma production. An analysis of the average currents for recorded-electron energies (4 – 20 keV) showed that the delay times were independent of the electron energy (to at least within 10 ns). These delays are in good agreement with the times of arrival at the secondary target for fast ions (H^+, C^+, Fe^{2+}) with energies of 26 keV per unit charge (130, 500, and 710 ns, respectively). It was noted that this energy coincided with the average ion energy measured in additional experiments. The electron current maxima are therefore due to the ionisation of strongly coupled electrons (primarily of K-shell electrons) under ion impact [22] and may be due to energetic negative ions produced in the plasma expansion and scattered at the surface of the secondary target [23, 24]. It is pertinent to note that the time of flight from the secondary target to the MCP via the spectrometer for electrons with energies above 14 keV is less than 4 ns.

Therefore, recording internal conversion electrons under the conditions of our experiment is possible in the range of 90 – 120-ns delays after plasma production. The electron spectrum obtained in this time range is plotted in Fig. 6. To calculate uncertainties, we investigated the statistical distribution of the electrons detected. Since the electron detection is a rare event (approximately one event per ten realisations), the realisations were combined in groups of 75, and a frequency histogram of the distribution was plotted from them, which was then compared with the Poisson distribution usually employed in nuclear physics (Fig. 7). For a quantitative measure of the similarity of the distributions we selected the Pirson criterion (χ^2). Its value calculated for our experimental data was equal to 0.87, which corresponds to a significance level of 0.08 (for this level, the quantile of the Pearson distribution $\chi^2_q = 0.93 > 0.87$). Therefore, the experimental distribution of the recorded electrons corresponds to the Poisson distribution with a probability of 92 %. All the uncertainties given in our work correspond to the confidence intervals of this distribution for a confidence level of 0.95.

The recorded spectrum peaks at energies of 5.6, 7.2, and 13.6 keV, which is in good agreement with the calculated spectrum (see Fig. 2). The peak widths are caused by the energy resolution of the spectrometer. Let us discuss the nature of these peaks separately. The peak in the energy

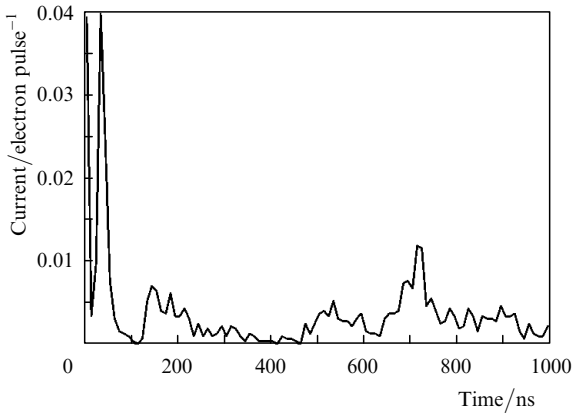

Figure 5. Typical dynamics of the electron current to the MCP.

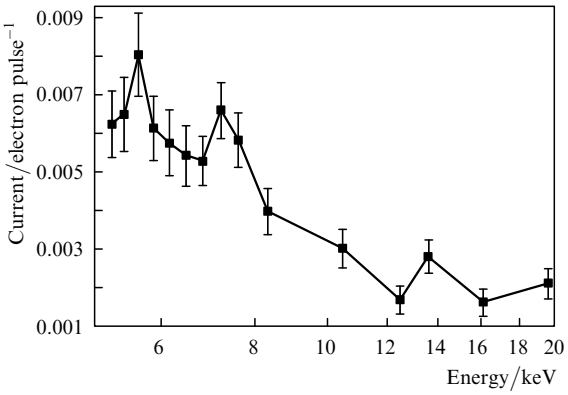

Figure 6. Electron spectrum in the 90 – 120-ns interval after plasma production; external target: ^{57}Fe.

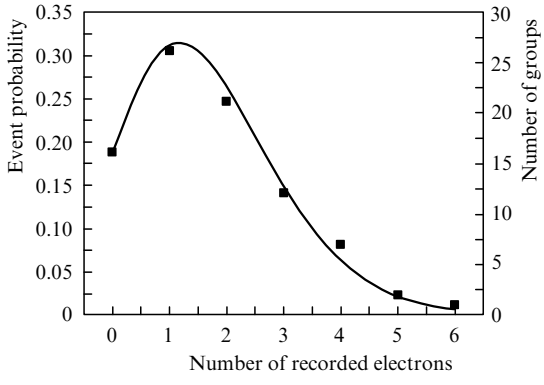

Figure 7. Frequency histogram of the distribution of recorded electrons.

spectrum near the 5.6 keV arises from the $K - L_2L_3$ transition, which fills the vacancy in the K shell. Such a vacancy may be produced in the K shell ionisation by plasma radiation as well as by way of internal electron conversion in the decay of the nuclear level of ^{57}Fe with an energy of 14.41 keV via this shell [25]. In principle, the energy peak near 7.2 keV may also be due to an atomic process: for instance, some K–MM transition. However, the probability of this Auger transition is extremely low in comparison with the $K - L_2L_3$ transition probability. That is why simultaneously with this peak there is bound to be a peak near the $K - L_2L_3$ transition energy (5.6 keV), and its amplitude should be many times higher than the amplitude of the peak about 7.2 keV. Since the amplitudes of the 5.6- and 7.2-keV energy peaks are about the same in our acquired spectra, it may be concluded that the 7.2-keV energy peak arises from the relaxation of the nuclear level of ^{57}Fe and the peak about 5.6 keV arises from the subsequent $K - L_2L_3$ transition.

The 13.6-keV peak in the energy spectrum cannot result from an Auger transition or some other atomic process. Indeed, the maximum electron binding energy in a Fe atom is equal to 7.1 keV (the K shell), and therefore the energy of an electron ejected by the atom due to interatomic intershell transitions cannot exceed this value. Consequently, the peak at this energy is attributable only to the decay of the nuclear level of ^{57}Fe. We emphasize that the ratio between the peaks corresponding to internal conversion via the K and L shells (7.2 and 13.6 keV) should be equal to ~ 2 (see Fig. 2). Our experimental data suggest that this ratio is 2.4 ± 0.9.

An additional substantiation of the fact that we do observe the internal electron conversion of the isomeric level of the ^{57}Fe isotope is the data given in Fig. 8c, which were obtained on replacing the ^{57}Fe-isotope target by a target of ordinary iron (the content of the ^{57}Fe-isotope is 2 % and that of the ^{56}Fe isotope is 98 %). It is pertinent to note that the first excited state of the ^{56}Fe-isotope nucleus has an energy of 847 keV [16]. As is evident from the data presented, no peaks are observed near 5.6 and 7.2 keV in this case.

The number of internal conversion electrons recorded in the case of the ^{57}Fe target may be estimated from the height of the 7.2-keV energy peak. Taking into consideration the geometry of our facility and the time interval of detection, our estimate suggests that for one laser pulse there are 1 ± 0.5 excited nuclei.

Since internal conversion electrons were observed in the time window 90–120 ns after the production of plasma at the primary target, the excitation of the isomeric level of the ^{57}Fe isotope with an energy of 14.41 keV may be due to either the photoexcitation by X-ray plasma radiation or to the excitation in the inelastic scattering of plasma electrons [8, 26, 27]. To reveal the main source of nuclei excitation we carried out an additional experiment, in which we placed a 20-μm-thick lavsan film in front of the secondary target to eliminate excitation by electrons. This film retained the electrons and ions emanating from the plasma at the surface of the first target and transmitted only hard X-ray photons. Indeed, from the Widdington–Thompson formula [28] we conclude that the free path of an electron with an initial energy of 14 keV in lavsan is equal to 3 μm. To calculate the ion free path, advantage is taken of the Bethe–Bloch model [28] for electron-induced deceleration. Then, for a proton with an initial energy of 26 keV the path to its complete

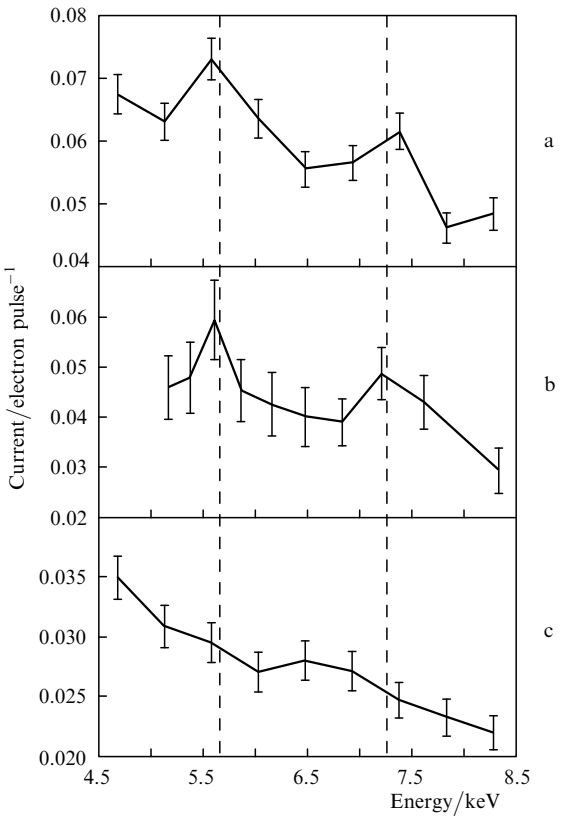

Figure 8. Electron spectra: with lavsan film placed in front of the ^{57}Fe secondary target, 50–140-ns interval after plasma production (a); without lavsan, 90–120-ns interval (b); without lavsan and with the secondary target of ^{56}Fe, 50–120-ns interval (c). The dashed lines correspond to the Auger peak (5.6 keV) and the internal conversion process (7.2 keV).

deceleration will be 1.3 μm, and much shorter for the rest of the ions accelerated in the plasma. The X-ray radiation is much weaker absorbed in lavsan (primarily due to photoeffect). The mass absorption coefficient for lavsan for a photon energy of 14 keV is equal to about 1.1 cm^2 g^{-1} [29]; for these photons, the absorption length turns out to be approximately equal to 1.5 cm. Consequently, in our experiment the excitation of nuclei in the secondary target may be attributed only to the photoexcitation mechanism.

The result of this experiment is presented in Fig. 8a. The time interval of spectra recording was widened to 50–140 ns, since neither the hot electrons from the plasma nor the protons could reach the secondary target and therefore did not produce the noise background for the electron current. In the electron spectrum one can clearly see the peaks at energies of 7.2 and 5.6 keV, which are attributable to the internal conversion electrons from the K shell and the attendant K–LL electrons, respectively. Taking into consideration the geometry of our facility and the time interval of detection, the number of nuclei excited in one laser pulse is estimated at 0.9 ± 0.3, which coincides, to within the experimental error, with the data derived in the experiment without lavsan. Therefore, photoexcitation is the principal excitation mechanism in our experiments, while the role of inelastic electron scattering is not clear and invites further investigation.

4. Conclusions

In the present work we have developed a new experimental approach to the problem of recording low-energy nuclear transitions with the use of laser-produced plasma. The hot dense plasma was produced by target irradiation by high-power femtosecond laser pulses. The fluxes of X-ray radiation and other fast plasma particles generated in this interaction irradiated the secondary target, which contained the ^{57}Fe isotope with an energy of the first excited state of 14.4 keV and a lifetime of 98 ns. The excited nuclear state decay was recorded from the energy spectra of the electrons emanating from the secondary target. The use of a two-target configuration in our experiment proved to be of significance in reducing the background irradiation of recoding instruments by the direct flux of plasma electrons. Furthermore, this configuration permits executing measurements with small amounts of the expensive isotope.

Our investigations have demonstrated that the electron energy spectra recorded for 90 – 120-ns delays after plasma production contained peaks corresponding to internal electron conversion involving the K and L shells of atomic iron in the isomeric nuclear transition from the 14.4-keV level in the ^{57}Fe isotope and to the corresponding $K - L_2L_3$ Auger transition. Additional investigations showed that the hard X-ray plasma radiation was the main source of excitation of the isomeric nuclear state; as this takes place, one nucleus is excited on average in the secondary target per one laser pulse.

It is noteworthy that the photoexcitation efficiency, which we estimated with the inclusion of laser-produced plasma luminosity for an excitation linewidth of the order of the radiative width of the nuclear transition, turned out to be several orders of magnitude lower than the indicated value. This, in particular, points to the significance of pursuing further experimental research and elaborating an adequate theory of the processes involved.

Acknowledgements. The authors express their appreciation to I.M. Band for the opportunity of using the programme package, to B.V. Mar'in for the prototype of electron spectrometer, and to A.V. Andreev and E.V. Tkalya for their fruitful discussions and criticism regarding the excitation mechanisms of isomeric states. This work would have hardly been possible without I.M. Lachko, who implemented the first version of the experimental facility.

This work was supported in part by the Russian Foundation for Basic Research under Grant Nos 09-02-12112-ofi_m and 10-02-01376a, and by the Ministry of Education and Science of the Russian Federation under State Contract No. 02.740.11.0223.

References

1. Andreev A.V., Gordienko V.M, Savel'ev A.B. *Kvantovaya Elektron.*, **31**, 941 (2001) [*Quantum Electron.*, **31**, 941 (2001)].
2. Ledingham K.W.D., McKenna P., Singhal R.P. *Science*, **300**, 1107 (2003).
3. Ledingham K.W.D., Galster W. *New J. Phys.*, **12**, 45005 (2010).
4. Gibbon P., Forster E. *Plasma Phys. Control. Fus.,* **38**, 769 (1996).
5. Mourou G.A., Tajima T., Bulanov S.V. *Rev. Mod. Phys.*, **78**, 309 (2006).
6. Andreev A.V., Gordienko V.M, Dykhne A.M., et al. *Pis'ma Zh. Eksp. Teor. Fiz.*, **66**, 331 (1997).
7. Andreev A.V., Volkov R.V., Gordienko V.M., et al. *Pis'ma Zh. Eksp. Teor. Fiz.*, **69**, 371 (1999).
8. Andreev A.V., Volkov R.V., Gordienko V.M., et al. *Zh. Eksp. Teor. Fiz.*, **118**, 1343 (2000).
9. Afonin V.I., Kakshin A.G., Mazunin A.V. *Fiz. Plazmy*, **36**, 273 (2010).
10. Andreev A.A., Van'kov A.K., Platonov K.Yu., et al. *Zh. Eksp. Teor. Fiz.*, **121**, 1004 (2001).
11. Izawa Y., Yamanaka C. *Phys. Lett. B*, **88**, 59 (1979).
12. Bol'shov L.A., Arutyunyan R.V., Strizhov V.F., et al. *Yad. Fiz.*, **53**, 36 (1991).
13. Malka G., Aleonard M.M., Chemin J.F., et al. *Proc. SPIE Int. Soc. Opt. Eng.*, **4510**, 58 (2001).
14. Claverie G., Aleonard M.M., Chemin J.F., et al. *Phys. Rev. C*, **70**, 44303 (2004).
15. Gobet F., Hannachi F., Aleonard M., et al. *J. Phys. B*, **41**, 145701 (2008).
16. http://www.nndc.bnl.gov/.
17. Band I.M., Fomichev V.I. Preprint of Leningrad Institute of Nuclear Physics No. 498 (Leningrad, 1979).
18. Drescher M., Hentschel M., Kienberger R., et al. *Nature*, **419**, 803 (2002).
19. Bol'shakov V.V., Vorob'ev A.A., Volkov R.V., et al. *Prikl. Fizika*, **1**, 18 (2009).
20. Gordienko V.M., Lachko I.M., Mikheev P.M., et al. *Plasma Phys. Control. Fus.,* **44**, 2555 (2002).
21. Volkov R.V., Gordienko V.M, Lachko I.M., et al. *Zh. Eksp. Teor. Fiz.*, **103**, 303 (2006).
22. Golovin G.V., Savel'ev A.B., Uryupina D.S., et al. *Pis'ma Zh. Eksp. Teor. Fiz.*, **89**, 584 (2009).
23. Volkov R.V., Gordienko V.M, Lachko I.M., et al. *Pis'ma Zh. Eksp. Teor. Fiz.*, **76**, 171 (2002).
24. Chutko O.V., Gordienko V.M., Lachko I.M., et al. *Appl. Phys. B*, **77**, 831 (2003).
25. Kawauchi T., Matsumoto M., Fukutani K., et al. *Rev. Sci. Instrum.*, **78**, 103303 (2007).
26. Tkalja E.V. *Laser Phys.*, **14**, 360 (2004).
27. Harston M.R., Chemin J.F. *Phys. Rev. C*, **59**, 2462 (1999).
28. Bobyl' A.V., Karmanenko S.F. *Fiziko-khimicheskie osnovy tekhnologii poluprovodnikov. Puchkovye i plazmennye protsessy v planarnoi tekhnologii* (Physicochemical Foundations of Semiconductor Technology. Beam and Plasma Processes in Planar Technology) (St.Petersburg: Izd. Politekhnicheskogo Universiteta, 2005).
29. Hubbell J.H., Seltzer S.M. *Tables of X-Ray Mass Attenuation Coefficients and Mass Energy-Absorption Coefficients 1 keV to 20 MeV for Elements Z = 1 to 92 and 48 Additional Substances of Dosimetric Interest* (Gaithersburg, MD: NIST, 1995).